FULL PAPER

Casimir Force Contrast Between Amorphous and Crystalline Phases of AIST

Gauthier Torricelli, Peter J. van Zwol, Olex Shpak, George Palasantzas,*
Vitaly B. Svetovoy, Chris Binns, Bart J. Kooi, Peter Jost, and Matthias Wuttig

Phase change materials (PCMs) can be rapidly and reversibly switched between the amorphous and crystalline state. The structural transformation is accompanied by a significant change of optical and electronic properties rendering PCMs suitable for rewritable optical data storage and nonvolatile electronic memories. The phase transformation is also accompanied by an increase of the Casimir force of 20 to 25% between gold and AIST ($Ag_5In_5Sb_{60}Te_{30}$) upon crystallization. Here the focus is on reproducing and understanding the observed change in Casimir force, which is shown to be related to a change of the dielectric function upon crystallization. The dielectric function changes in two separate frequency ranges: the increase of absorption in the visible range is due to resonance bonding, which is unique for the crystalline phase, while free carrier absorption is responsible for changes in the infrared regime. It is shown that free carriers contribute ≈50% to the force contrast, while the other half comes from resonance bonding. This helps to identify PCMs that maximize force contrast. Finally it is shown that if this concept of force control is to be employed in microelectromechanical devices, then protective capping layers of PCMs must be only a few nanometers thick to minimize reduction of the force contrast.

1. Introduction

Casimir forces[1–12] arise between two surfaces due to a perturbation of the quantum zero-point energy of the electromagnetic field. Adjacent surfaces restrict the allowed wavelengths and thus the number of field modes within the cavity. This locally depresses the zero point energy of the electromagnetic field. The reduction of the number of modes depends on the separation between the plates. Thus there is a force between them, which for normal materials is always attractive if the medium in the cavity is air or vacuum.[1] In the small separation limit this gives rise to the familiar van der Waals force.

The original calculation of the Casimir force assumed two parallel plates with infinite conductivity.[1] This was later modified to include the dielectric properties of real materials and the intervening medium.[2,3] These extensions have provided the first glimpse of possible methods to control the magnitude and even the direction of the Casimir force. This finding has motivated our attempts to manipulate the dielectric properties of a material and hence generate force contrast.[9–13] A particularly attractive possibility is to produce a "switchable" Casimir force between a high and low force state by employing materials whose optical properties can be changed in situ in response to a simple stimulus. This requires a large modification of the dielectric response upon a phase transformation in this material to obtain a large Casimir force contrast. Besides significant force contrast between different materials,[11] the modification of the Casimir force with carrier density was also studied in semiconducting materials.[10,13] Interesting enough, in a recent study a significant decrease in the magnitude of the Casimir force of ≈21–35% was observed, after an indium tin oxide (ITO) sample interacting with an Au sphere was subjected to UV treatment.[14] The corresponding modification of the optical properties of the film was shown[14] to be insufficient to change the Casimir force sufficiently, if Lifshitz theory is applied. This is in striking contrast with the data presented here for the phase change material $Ag_5In_5Sb_{60}Te_{30}$ (AIST), where the incrase of Casimir force upon crystallization is in line with the predictions of Lifshitz theory.

Here, we explain the origin of the change in Casimir force upon crystallization. Phase change materials are renowned for the rapid and reversible switching between the amorphous and crystalline phase,[15–33] which has already been used for more than two decades in rewriteable optical data storage,[15–17,25–31]

Dr. G. Torricelli, Prof. C. Binns
Department of Physics and Astronomy
University of Leicester
Leicester LE1 7RH, UK

Dr. P. J. van Zwol, O. Shpak, Dr. G. Palasantzas,
Prof. B. J. Kooi
Zernike Institute for Advanced Materials
University of Groningen
Groningen, 9747 AG, The Netherlands
E-mail: g.palasantzas@rug.nl

Dr. V. B. Svetovoy
MESA+ Institute for Nanotechnology
University of Twente
Enschede, 7500AE, The Netherlands

P. Jost, Prof. M. Wuttig
I. Physikalisches Institut (IA) and JARA-FIT
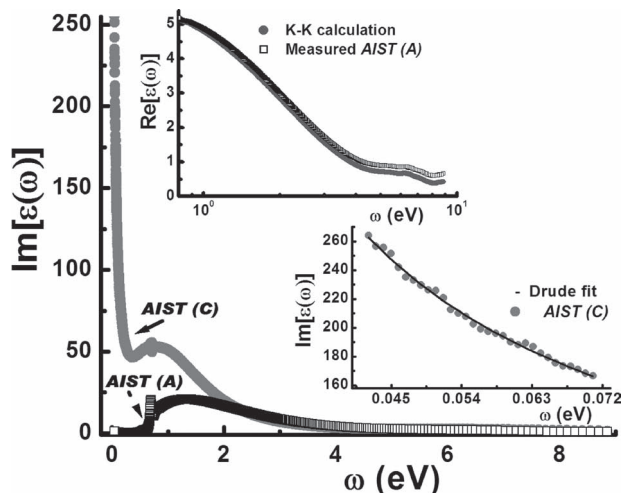RWTH Aachen University
52056 Aachen, Germany

Figure 1. Absorptive part of the dielectric function for the crystalline (red circles) and amorphous (solid line-squares) state of the AIST film obtained from spectroscopic ellipsometry data. The upper inset shows the Kramers-Kronig (K-K) consistency for the real part of the dielectric function of amorphous AIST. The lower inset shows the fit of optical data for crystalline AIST (C) by the Drude model (see Equation (1)).

where the pronounced optical contrast between the amorphous and crystalline state (**Figure 1**) is employed to store information. Using an intense focussed laser beam the phase change material is heated above the melting temperature. Rapid quenching of the liquid material produces a glass-like amorphous state. The amorphous phase has a markedly lower reflectivity and can hence easily be distinguished form the more reflective crystalline state. Upon heating the amorphous phase change material by a focused laser beam with moderate intensity the amorphous state reverts to the more stable crystalline phase. This principle has already been successfully employed in three generations of rewriteable optical data storage devices (CD-RW, DVD-RW, and BD-RW, where RW stands for "re-writeable"). The good cyclability of phase change materials ensures the realization of a switchable Casimir force device.

An increase in the force by up to 20–25% between gold and AIST surfaces was measured upon crystallization of an amorphous sample of AIST.[12] The change in Casimir force has been attributed to a change of the dielectric (optical) properties upon crystallization. This structural transformation, however, leads to changes of the optical properties in two well separated frequency ranges. Crystallization of phase change materials is accompanied by the formation of resonance bonds. This change of bonding mechanism affects the optical properties in the visible and ultraviolet frequency range. The corresponding contrast of the properties between the amorphous and crystalline state is exploited in rewritable optical data storage employing phase change materials. So far, no second class of materials has been identified, which encompasses a similar change of optical properties upon crystallization. If it can be proven that the change of optical properties in the visible range is decisive for the Casimir force contrast, then it can be concluded that phase change materials form a very promising and unique material class to maximize Casimir force contrast.

In many phase change materials, however, crystallization also leads to the generation of a large amount of free carriers. These carriers produce a concomitant change in the infrared frequency range of the dielectric function. Hence it is crucial to understand if the change of Casimir force upon crystallization is mainly due to the change of the dielectric function in the infrared regime (free carriers) or in the visible range (resonance bonding). Only when this question has been answered, it is possible to devise a strategy how to identify phase change materials which optimize the Casimir force contrast upon crystallization. Furthermore it is crucial that the force contrast can be utilized in actual devices. To enable this, it is helpful if the phase change material can be covered by a dielectric coating that would protect the underlying phase change material from chemical reactions with the environment and allows melting without disturbing shape changes. Hence, we have studied how protective dielectric coatings can be utilized to realize a potential switchable Casimir force device.

2. Analysis of Optical Properties

To understand the difference in the Casimir force (**Figure 2**) between the amorphous and the crystalline state,[12] it is necessary to determine the dielectric function over a large frequency range (Figure 1). This has been accomplished by measurements from the far infrared (IR) up to the ultraviolet (UV) range employing spectroscopic ellipsometry measurements.[12] Subsequently, the measured optical spectra have been fitted to obtain the dielectric function. As Figure 1 shows, the amorphous AIST film is transparent in the IR range, but is optically thick in the visible and UV range. Therefore, the optical properties of the Al substrate are only important in the IR range, where tabulated data for the dielectric function of Al were used. The crystalline phase change film has to be modeled by a dielectric function that differs
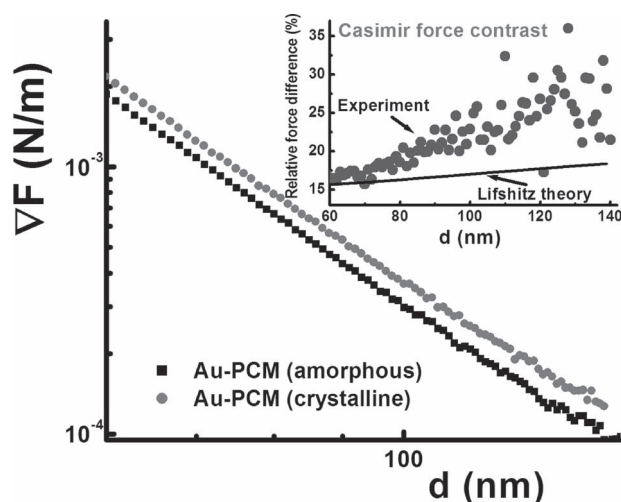

Figure 2. Casimir force gradient measurements are shown for the crystalline and amorphous AIST at separations d > 60 nm where surface roughness has no influence. The inset shows the relative force difference, normalized with respect the amorphous state, for both the experiment as well as the prediction of Lifshitz theory.

considerably from the corresponding one for the amorphous state. This is due to the fact that i) the bonding in the crystalline state of phase change materials differs from its counterpart in the amorphous state[25–28] and ii) a significant number of free carriers exist in the crystalline state of many phase change materials.[26]

Crystalline phase change materials are characterized by the so-called resonant bonding,[25–28] which can only prevail if the corresponding material is not too ionic and the hybridization between the s- and p-type valence electrons is small.[15] Under these circumstances bonding via the p-electrons prevails and on average approximately three electrons are available to stabilize the six-fold coordination.[28] In the crystalline state, the p-orbitals of adjacent atoms are sufficiently well aligned to enable resonant bonding. This alignment is missing in the amorphous state, hence resonant bonding cannot occur here.[25] The unique bonding mechanism in the crystalline state has a pronounced influence on the dielectric function. Resonant bonding leads to a strong increase in the intensity of optically excited interband transitions and hence a strong absorption.[16] These interband transitions can only occur above the band-gap between the valence and the conduction band. In phase change materials, this band gap is often of the order of ≈0.5–1.0 eV. Hence this change of the dielectric function is relevant for optical data storage, where photon energies between approximately 1.5 eV (compact discs) and 3 eV (blu-ray disk) are employed. In amorphous phase change materials the lack of long range order prevents the alignment of adjacent p-orbitals,[25] leading to much weaker absorption and hence very different dielectric function.

However, there is often a second difference between the amorphous and the crystalline state, which has consequences for the dielectric function as well. Frequently the crystalline phase shows metallic behavior,[25] which is not the case for the amorphous state. This metallic behavior is somewhat surprising at first sight. Often, phase change materials such as GeTe or also Ge$_1$Sb$_2$Te$_4$ or Ge$_2$Sb$_2$Te$_5$ have 3 p-electrons per site. Therefore the corresponding p-band is half filled. Employing Hund's rule this gives rise to a stable electronic configuration[15–17,32] and should lead to a band gap between the occupied, bonding p-states, and the empty, anti-bonding p-states. Indeed, density functional theory (DFT) calculations for the phase change materials listed above typically produce such a band gap. Experimentally, however, these crystalline phase change materials often show metallic behavior, where the Fermi energy is located in the valence band. This has been explained for GeTe,[33] where DFT calculations reveal, that it is favorable to form vacancies on the Ge sub-lattice. These vacancies help to pin the Fermi energy close to, but below the valence band edge. A similar mechanism seems to be at play also for more complex, ternary phase change materials such as Ge$_1$Sb$_2$Te$_4$ or Ge$_2$Sb$_2$Te$_5$. In these phase change materials with increasing annealing temperature a transition is observed in the crystalline state, where the electrical conductivity changes from nonmetallic to metallic. This remarkable transition has been identified as an Anderson-like delocalization process of the charge carriers at the Fermi energy.[25–28] Hence, in such ternary materials we can even modify the conductivity within the crystalline state. The metallic behavior observed for many crystalline phase change materials leads to an additional contribution to the dielectric function and as a result to the Casimir force contrast.

To incorporate the contribution of mobile charge carriers we have to include a Drude contribution to the dielectric function of the crystalline state, which has been discussed in detail previously.[26] In this state phase change materials are typically characterized by a large number of free carriers (≥10^{20}/cm^3 depending on the PCM material).[26] At the same time, they usually possess only very small mean free paths, which are often even below ≈3 nm.[26] The Drude model, which was fitted to the optical data for the crystalline state (lower inset in Figure 1) has the form:

$$\varepsilon(\omega) = C - \frac{\omega_p^2}{\omega(\omega + i\omega_\tau)} \tag{1}$$

as also used in other studies of the Casimir force,[5,8,10,34] where ω_p is the plasma frequency, and ω_τ is a damping term due to absorption of electromagnetic radiation. For the amorphous state the IR and far-IR (below 0.04 eV) energy range has no effect on the Casimir force (the material is transparent). Because absorption is small at high frequencies ($\omega > 8.9$ eV), the imaginary part $\varepsilon(\omega)$ of the dielectric function in this frequency range was extrapolated as ≈$1/\omega^3$.[12]

For the crystalline AIST ω_τ is large (as it is reflected by the small mean free paths for PCM materials). Hence these materials often do not show a clear plasma edge so that it is impossible to derive both ω_τ and ω_p. If we restrict ourselves to frequencies $\omega << \omega_\tau$, the Drude model obtains the simpler form $\varepsilon(\omega) = C + i(\omega_p^2/\omega\omega_\tau)$ but fitting yields only the constant C and the ratio ω_p^2/ω_τ. The latter is related to the optical conductivity $\sigma = \varepsilon_0(\omega_p^2/\omega_\tau)$ with ε_o the permitivity of vacuum. By fitting the crystalline AIST data with the Drude model in the frequency range below 0.07 eV, see lower inset in Figure 1, we have obtained C = 51 and ω_p^2/ω_τ = 10.6 eV. The latter yields a value for the conductivity $\sigma \approx 1.4 \times 10^5$ (Ω m)$^{-1}$ or a resistivity $\rho \approx 7 \times 10^{-6}$ (Ω m). If we compare the latter to metals where $\rho \approx 10^{-7}$ (Ω m) then the resistivity of crystalline AIST is more than an order of magnitude higher. This is due to the smaller number of charge carriers, which has been determined by Hall measurements to $N_{AIST} \approx 2 \times 10^{21}$/cm^3.[26] In addition, these measurements revealed a mobility of ≈5 cm^2/V s.

To determine the influence of the free carriers on the Casimir force contrast, we have simply subtracted it from the total contribution for the dielectric function (**Figure 3**). Subsequently, the Casimir force has been calculated using Lifshitz theory. The inset of Figure 3 shows the dielectric function at imaginary frequencies $\varepsilon(i\zeta)$,[2,3]

$$\varepsilon(i\zeta) = 1 + \frac{2}{\pi} \int_0^{+\infty} \frac{\omega\varepsilon''(\omega)}{\omega^2 + \zeta^2} d\omega \tag{2}$$

which is necessary for the force calculations. Subtracting the Drude contribution already has a pronounced effect on $\varepsilon(i\zeta)$, as can be seen in the inset of Equation (2) and to subsequently derive the Casimir force via Lifshitz theory,[2,3,34] it is necessary to extrapolate the optical data to higher frequencies. The quality of this extrapolation is validated by the good Kramers-Kronig (K-K) consistency

$$\varepsilon'(\omega) = 1 + \frac{2}{\pi} P \int_0^{\infty} \frac{x\varepsilon''(x)}{x^2 - \omega^2} dx \tag{3}$$
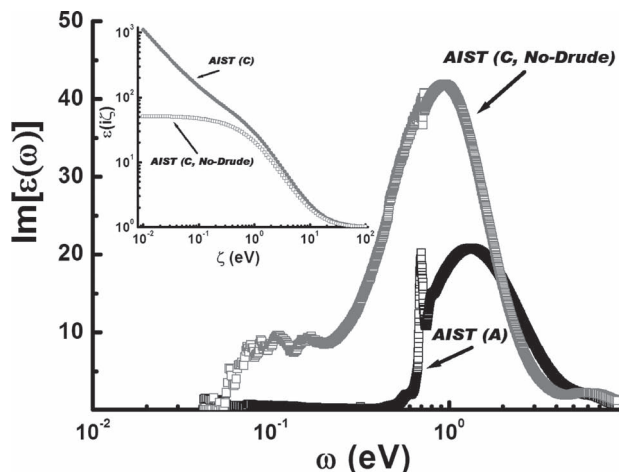
Figure 3. Optical absorption data for AIST with the Drude contribution from Figure 2 removed (No-Drude). The inset shows calculation of the functional $\varepsilon(i\zeta)$, which is important for Casimir force calculations via Lifshitz theory with and without the Drude contribution.

with P indicating the principal part of the integral for both the amorphous and crystalline films (e.g., upper inset in Figure 1). An even better K-K consistency could be achieved if experimental data beyond 8.6 eV would be known. Good agreement was also found with the permittivities of the films obtained in former studies.[25–28] The measured dielectric response allows Casimir force calculations (Figure 2) using the Lifshitz theory,[2,3] assuming flat surfaces. Indeed, as previous studies have shown, nanoscale rough surfaces have a negligible influence on the Casimir force at relatively large separations (>60 nm).[35] Since the typical roughness of the AIST samples was a few nm rms (root mean square), but with a few isolated local peaks as evidenced by atomic force microscopy (AFM) analysis,[12] this assumption is justified for a qualitative comparison with measured force data.

Calculations of the Casimir force contrast, **Figure 4**, show that without the Drude contribution this contrast only reaches a level of 10%, whereas it increases significantly with the Drude
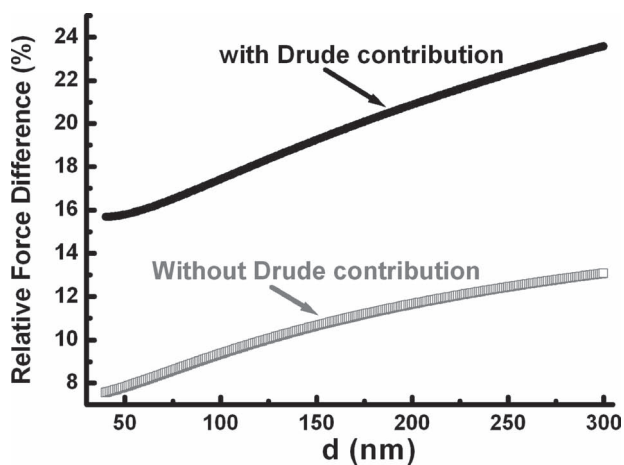

Figure 4. Casimir force contrast calculations based on optical data with and without Drude contribution for the crystalline AIST film.

component. While the IR absorption due to free charge carriers is responsible for approximately 50% of the force contrast, resonant bonding, which dominates the absorption in the visible to ultraviolet range is responsible for the remaining 50% of the force contrast. Hence, the change of bonding mechanism upon crystallization and the accompanying formation of free carriers contribute almost equally to the force contrast. As mentioned before, the formation of resonance bonds in the crystalline state is a fingerprint of phase change materials.[25–28] Hence the contribution to the change of the dielectric function in the visible to UV range to the Casimir force contrast is a unique feature of phase change materials that cannot be exploited in other materials such as metals, insulators or ordinary covalent semiconductors.[15] This indicates that it will be difficult to find other material classes which possess an equally pronounced change of Casimir force upon crystallization. The conclusion also raises the question if phase change materials can be identified, where the contribution of resonance bonding in the crystalline state is particularly pronounced. A tentative answer to this question has already been given. Lencer et al.[15] have recently derived a first map for phase change materials which presents the necessary framework to discuss systematic property trends as a function of stoichiometry. As discussed in this paper, resonance bonding can only prevail, if the bonding is not too ionic and only a weak hybridization between s- and p-states prevails. This helps to identify candidates where resonance bonding in the crystalline state and hence the corresponding contribution to the Casimir force contrast should be particularly pronounced.

As shown above, the second and equally important contribution to the Casimir force contrast comes from the free carriers. Upon crystallization, many phase change materials reveal a metallic conductivity, which leads to a pronounced Drude contribution. In a recent publication it has been shown, however, for a number of phase change materials that the Drude contribution of the crystalline phase can vanish, if the crystalline state is characterized by a significant degree of disorder.[26] This disorder can be so pronounced, that the crystalline phase even becomes insulating, i.e., has a negative temperature dependence of the electrical resistivity. For such a material, the absence of free carriers due to disorder induced localization also leads to the absence of a Drude contribution. For such a phase change alloy we hence expect a significantly smaller Casimir force contrast. This gives us two strategies to maximize the force contrast upon crystallization of phase change materials: employ materials with particularly strong resonant bonds, as found in phase change materials with low iconicity and small average hybridization of s- and p-states, as well as small disorder and large carrier concentration to ensure a large Drude contribution.

3. Analysis of Force Measurements

Prior to the force measurements in AIST films (Figure 2),[12,36] the measurement set-up was tested by independent force measurements between Au coated spheres and Au thin films. As **Figure 5** indicates the force gradient scales qualitatively with separation distance as an average power law $\nabla F \sim d^{-3.61}$. This implies that the force scales as $F \sim d^{-2.61}$. In a strict sense the Casimir force shows a more complex behavior, where the local
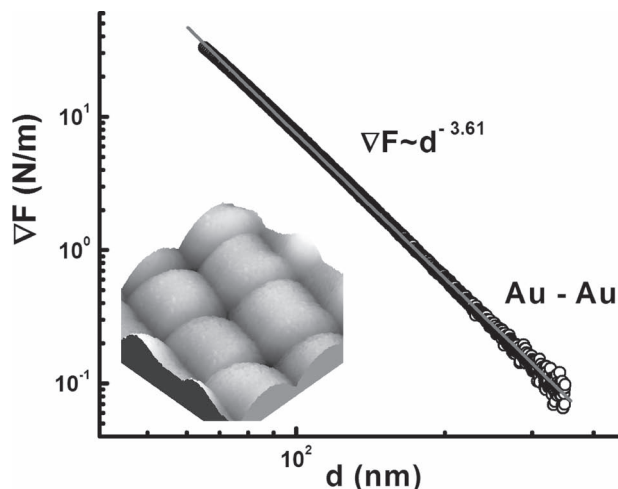
Materials
Views
www.MaterialsViews.com

ADVANCED
FUNCTIONAL
MATERIALS
www.afm-journal.de

FULL PAPER

Figure 5. Casimir force gradient measurement between an Au coated plate and the Au coated sphere used for the force measurements of the AIST films. The error of the measured exponent is less than 0.05. The inset depicts an inverse AFM image (vertical scale 0–85 nm, lateral size 6×6 µm^2; obtained by scanning the sphere onto a grid of inverted sharp tips) of the Au coated sphere.
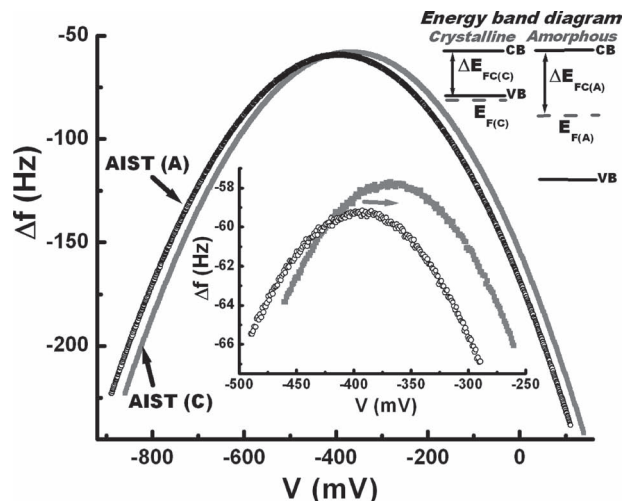

Figure 6. Frequency shift of the resonator versus applied potential. This yields a parabola with a maximum when the contact potential between gold and AIST is minimized. The lower inset shows in more detail the electrostatics curves around the maximum. The contact potential difference for the amorphous and crystalline phases as depicted by the shift of the maxima (arrow in the inset) is ≈25 mV. The upper inset shows an approximate band diagram for the amorphous and crystalline PCM that allows qualitative estimation of the Fermi level difference.

value of the exponent varies with separation distance towards the asymptotic values 3 (which is typical for perfectly reflecting mirrors) for separations typically > 1 µm. This scaling exponent is in close agreement with independent findings of past force measurements between relatively flat Au surfaces.[35] Notably, as the inset of Figure 5 shows the Au coated spheres (imaged using inverse AFM)[38] were very clean after Au deposition having roughness peaks of at most 6 nm in height.

Having established that the force set-up is working properly, to perform a precise comparison of force measurements with theory several parameters have to be determined. These are the starting separation distance Z_0, for the force measurement (corresponding here to the shortest separation), the cantilever spring constant k, and the contact potential difference V_0 (**Figure 6**).[36] The electrostatic calibration is performed by measuring the force gradient versus separation distance for two different applied bias voltages V_b on the sphere yielding a gap voltage $\Delta V = V_b - V_0$. The contact potential V_0 may not be constant[11,36,39,40] but instead can depend on the separation distance Z between sphere and sample surface. Before data acquisition, the determination of V_0 is performed at only one distance $Z_0 = 42.8 \pm 0.5$ nm for the amorphous, and $Z_0 = 42.9 \pm 0.4$ nm for the crystalline AIST sample. In order to perform the electrostatic calibration V_b is then chosen so that $\Delta V = 0.5$ V and $\Delta V = -0.5$ V at $Z = Z_0$.[36] The values of Z_0 and the spring constant k are obtained by fitting the average of the two electrostatic force measurements after subtraction of the Casimir contribution ($\Delta V = 0$ V).[36] Using this procedure the calibration is not affected by variations in V_0.[36] This procedure leads to consistent spring constants of $k = 10.8 \pm 0.3$ N/m and $k = 10.7 \pm 0.3$ N/m upon measuring amorphous and crystalline AIST films, respectively.

The fit for the determination of Z_0 was stable (with chi-square ≈0.9999 and R-square ≈0.05) within the separation range used for the force measurements. In addition, the error δZ_0 in

determing Z_0 by fitting different sections of the electrostatic curves was within the error bars of Z_0. If we set $\delta Z_0 \approx 0.5$ nm then we have $\delta Z_0 / Z_0 \approx 0.01$ yielding only a small relative error for the Casimir force $\delta F_0 / F \approx 2.4(\delta Z_0 / Z_0) \approx 0.02$ (≈ 2%). The latter was estimated by taking into account the average power law behavior of the Casimir force, which is shown in **Figure 7**. Indeed, for surface separations d > 50 nm where the surface roughness ceases to play any significant role, we have determined a power law dependence of the force gradient, as in Figure 5, on surface separation for both the amorphous and the crystalline sample of the form $\nabla F \sim d^{-(1+m)}$. The exponents obtained from the linear fits are $m_{Au-cryst.} = 2.43$ and $m_{Au-amor.} = 2.49$, respectively, while for Au-Au surfaces it is found to be $m_{Au-Au} = 2.61$. For the AIST surfaces, the exponent is in both cases slightly lower but still close to the value for Au–Au surfaces (in the separation range $d \approx 20$–100 nm).[35] This power law behavior demonstrates that the error $\delta F_0 / F$ due to the uncertainty in Z_0 is much smaller than the Casimir force contrast and thus does not affect our conclusions.

Furthermore for the Casimir force measurement the value of the applied voltage V_b is chosen so that $\Delta V = 0$ V at $Z = Z_0$. Nevertheless, there is still a residual electrostatic force present which scales as $\approx V_0(Z)^2$ and must be subtracted from the measured force. $V_0(Z)$ can be extracted from two electrostatic measurements ($\Delta V = \pm 0.5$V) by simple data manipulation.[36] For both samples, similar variations of $V_0(Z)$ between 0 and 20 mV were observed for sphere-plate separations ≈40–150 nm.[12] Since the residual electrostatic interaction is similar for both samples it does not affect the comparison of the Casimir force measurement between the two phases of the AIST films (Figure 2). As Figure 6 shows the frequency shift of the resonator versus applied potential yields a parabola with a maximum when the contact potential between gold and AIST is minimized.[36] The
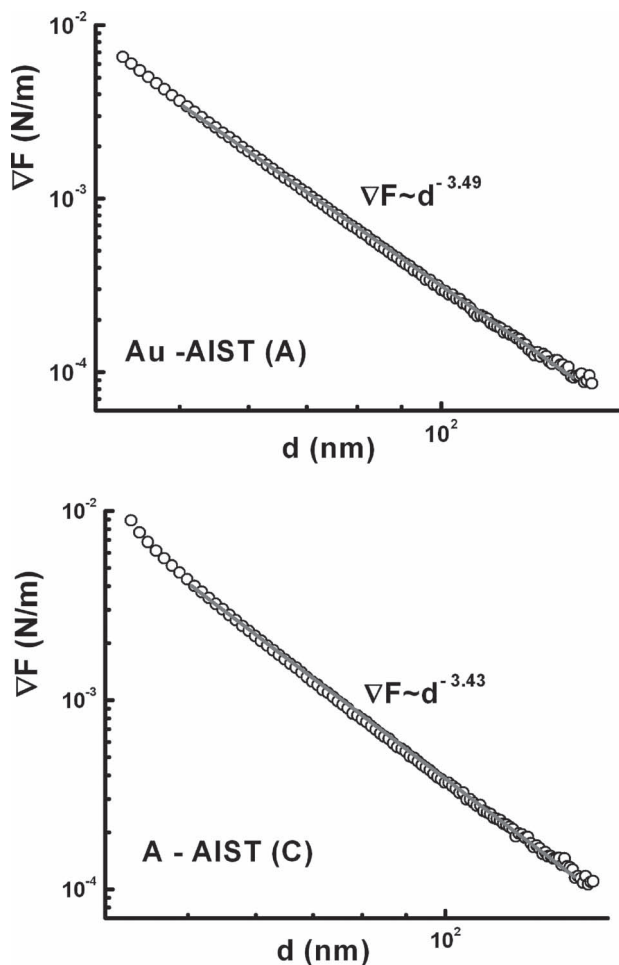
Figure 7. Determination of the power-law exponent for both the crystalline (bottom) and the amorphous (top) AIST films in the separation range between 55 and 130 nm. The error of the measured exponent is less than 0.05.

maximum position yields the actual value of V_0.[36] The contact potential difference for the amorphous and crystalline phases, as depicted by the shift of the maximum in Figure 6, is $\Delta V_0 \approx$ 25 mV. Note that although the measured contact potential difference V_0 between the Au-crystalline and the Au-amorphous AIST was slightly different, it does not affect the comparison between both force curves of Figure 2 because V_0 was compensated in both cases.

It remains, however, a nontrivial issue to understand the origin of the contact potential difference $\Delta V_0 \approx$ 25 mV between the amorphous and crystalline AIST. The amorphous phase behaves like an ordinary semiconductor where the Fermi energy is located in the middle of the band gap of $\Delta E_{FC(A)} \approx 0.32$ eV (upper inset Figure 6) below the conduction band edge.[25–28] The crystalline phase has, however, the Fermi energy in the valence band since it has p-type conductivity. The upper edge of the valence band (with the Fermi level just below the edge of the valence band) in crystalline AIST is $\Delta E_{FC(C)} \approx 0.2$ eV below the lower edge of the conduction band (upper inset Figure 6).[25–28] If we consider as a reference energy level the lower edge of the

conduction band for both states, then the difference in the position of the Fermi energy is $\Delta E_F \approx \Delta E_{FC(A)} - \Delta E_{FC(C)} \approx 0.1$ eV (see upper inset Figure 6). On the other hand scanning surface potential microscopy (SSPM) analysis of crystalline-amorphous interfaces of PCM materials indicated changes of the surface potential in the range ≈40–100 mV. These values are not significantly different from the observed shift of the electrostatic curves. This indicates that the origin of the shift is possibly due to differences in the density of electronic states of amorphous and crystalline AIST.

For the Casimir force contrast (Figure 2) it is crucial to estimate the influence of this residual electrostatic contribution. Subtraction of this contribution corresponds to a correction of 6% at Z = 150 nm, while it is much less than 1% at Z = 50 nm as compared to the Casimir force.[12] These estimates indicate that in the range from 50 to 150 nm the force contrast that occurs during a phase transition is dominated by the genuine Casimir interaction. Furthermore, the experimental uncertainty in the force measurement as deduced from the standard deviation of the cantilever spring constant k and the starting separation distance Z_0 is about 7% for both samples. Therefore, the Casimir force increases in relative magnitude by approximately 20–25% as a result of crystallization, in good qualitative agreement with theoretical calculations.[12] The observed force contrast is much larger than any possible error.

4. Analysis of the Influence of Capping Layer on Force Contrast

The property portfolio of suitable dielectrical properties, fast switching,[29,30] good scalability down to the nanometer regime,[29,30] and strong Casimir force contrast (Figure 2) deem PCM a particularly promising candidate for a switchable force device, i.e., in actuation of micro/nanoelectromechanical systems (MEMS/NEMS).[6–8] However, for in situ switching phase-change materials, capping layers are required to protect phase change films against for instance oxidation. Such a protective capping would also help to protect the phase change film against shape changes and material loss, when it is transformed from the crystalline to the amorphous state via the liquid phase. Indeed, in optical rewriteable data storage, such capping layers have enabled the development of storage media employing the reversible switching of phase change films with a large number of cycles. Without loss of device performance such disks could be switched up to a million times. The required capping layers should be transparent and non conductive like SiO_x. In order to understand the influence of this type of capping layers, **Figure 8** shows force contrast calculations using the Lifshitz theory[2,3] for the Au-AIST system. The force calculations were performed for silica (SiO_2) capping layers with a thickness of 5 and 10 nm respectively, using measured optical properties for SiO_2 as input for the Lifshitz theory.[41]

The results in Figure 8 demonstrate that the capping layers decrease the force contrast significantly. Therefore, for future applications, aiming to control the Casimir force in micro/nanotechnologies[32] using PCMs, the protective capping layer must be uniform and thinner than 5 nm. Alternatively, another PCM has to be found that provides higher contrast to
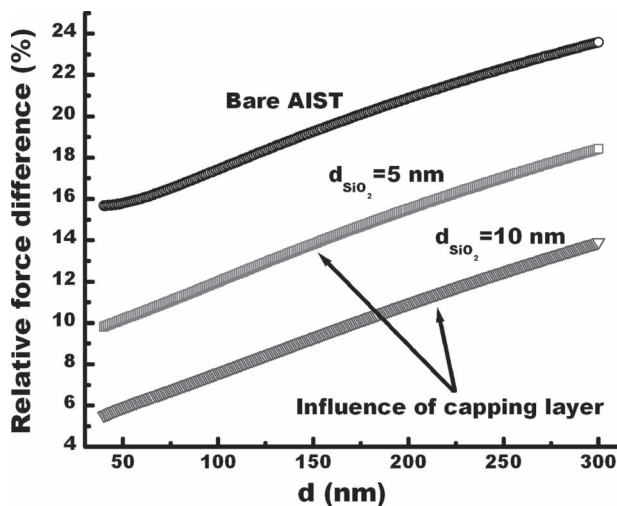
www.MaterialsViews.com

ADVANCED
FUNCTIONAL
MATERIALS
www.afm-journal.de

FULL PAPER

Figure 8. Calculated relative Casimir force contrast $(F_{cryst} - F_{amorph})/F_{amorph}$ using measured optical properties for bare AIST, and for AIST with protective layers of silica, which are, respectively, 5 nm and 10 nm thick.

nano-engineers because it obstructs the operation of MEMS, a tunable Casimir force could help to alleviate these problems by switching from high to low force state and allow microcomponents to be released.[6–8]

6. Experimental Section

Film Preparation and Optical Characterization: For the measurement of Casimir forces in PCMs, we have sputter deposited 1 μm thick amorphous AgInSbTe (AIST: $Ag_5In_5Sb_{60}Te_{30}$)[24] thin films onto standard Al coated (in-situ with the AIST films) Si wafers, of which half of the AIST films (from the same batch) were annealed to the crystalline state. Subsequently, the samples were optically characterized by ellipsometry in the frequency range from 0.04 to 8.9 eV as shown in Figure 1. The ellipsometry measurements were performed at two angles of incidence of $\theta_1 = 60°$ and $\theta_2 = 75°$.

Force Measurements: Casimir force measurements, shown in Figure 2, were performed using a dynamic mode within an ultra high vacuum (UHV) Atomic Force Microscope (Omicron VT STM/AFM).[34] Forces were measured in the sphere-plate geometry between an Au coated (100 nm thick) sphere 20.2 μm in diameter as determined by SEM (the spheres have a NIST-traceable diameter within ≈1.5% variation), attached at the end of a cantilever. The latter initially vibrates at its resonant frequency, $f_o = 83.6 \pm 0.003$ kHz, far away from the surface. As the sphere approaches the AIST surface, the frequency shift induced by the sphere-plate interaction is measured, which is proportional to the force gradient (∇F) in the linear approximation; $\Delta f = (f_o/2k)\nabla F$ with k the cantilever spring constant.[36] Each experimental force curve is an average of 13 measurements taken at different areas on both samples.

compensate for the reduction of the Casimir force upon capping. Such nonconductive capping layers will also contribute to electrostatic charging, which could be detrimental for the Casimir force contrast, if both states charge differently. This is an issue which requires further investigation to secure the application potential of phase change materials in micro- and nanomechanical devices employing Casimir force contrast.

5. Conclusions

The pronounced difference in the dielectric properties between the amorphous and crystalline states in phase change materials leads to a significant difference in the measured Casimir force between the two phases. This change in optical properties is caused by the strong absorption of electromagnetic radiation by free charge carriers and resonance bonding, both present in the crystalline phase. This finding demonstrates that in phase change materials two different mechanisms can give rise to a contrast of the Casimir force. Our investigation reveals that for AIST both contributions are almost equally important. This insight will help to identify phase change materials with superior Casimir force changes upon crystallization since it establishes a clear recipe which phase change materials to look for.

For in situ applications of phase change materials, protective capping layers will be required. These layers need to be sufficiently thin to minimize the reduction of the force contrast to ensure proper device operation by switching between high and low Casimir force states. This is a unique feature that is not present for electrostatic actuation if no voltage is applied. Switching between high-low force states by switching between crystalline-amorphous states enables the control of MEM/NEM actuation dynamics in smart ways leading to development of ultrasensitive force and torque sensors, which can levitate objects above surfaces without disturbing electric/magnetic interactions and virtually no static friction to rotation or translation. Finally since stiction is a growing problem for micro/

[1] H. B. Casimir, *Proc. K. Ned. Akad. Wet.* **1948**, *51*, 793.
[2] E. M. Lifshitz, *Sov. Phys. JETP* **1956**, *2*, 73.
[3] I. E. Dzyaloshinskii, E. M. Lifshitz, L. P. Pitaevskii, *Sov. Phys. Usp.* **1961**, *4*, 153.
[4] a) S. K. Lamoreaux, *Phys. Rev. Lett.* **1997**, *78*, 5; b) S. K. Lamoreaux, *Rep. Prog. Phys.* **2005**, *68*, 201.
[5] M. Bordag, U. Mohideen, V. M. Mostepanenko, *Phys. Rep.* **2001**, *353*, 1.
[6] a) S. K. Lamoreaux, *Phys. Today* **2007**, *60*, 40; b) A. Lambrecht, *Nature* **2008**, *454*, 836; c) A. W. Rodriguez, F. Capasso, S. G. Johnson, *Nat. Photonics* **2011**, *5*, 211.
[7] F. Capasso, J. N. Munday, D. Iannuzzi, H. B. Chan, *IEEE J. Sel. Top. Quantum Electron.* **2007**, *13*, 400.
[8] a) H. B. Chan, V. A. Aksyuk, R. N. Kleiman, D. J. Bishop, F. Capasso, *Phys. Rev. Lett.* **2001**, *87*, 211801; b) A. Roy, U. Mohideen, *Phys. Rev. Lett.* **1999**, *82*, 4380; c) B. W. Harris, F. Chen, U. Mohideen, *Phys. Rev. A.* **2000**, *62*, 052109; d) H. B. Chan, V. A. Aksyuk, R. N. Kleiman, D. J. Bishop, F. Capasso, *Science* **2001**, *291*, 1941; d) R. Decca, E. Fischbach, G. L. Klimchitskaya, D. E. Krause,

FULL PAPER

D. López, V. M. Mostepanenko, *Phys. Rev. D* **2003**, *68*, 116003;
f) R. S. Decca, D. López, E. Fischbach, G. L. Klimchitskaya,
D. E. Krause, V. M. Mostepanenko, *Phys. Rev. D* **2007**, *75*, 077101;
g) R. S. Decca, D. López, E. Fischbach, G. L. Klimchitskaya,
D. E. Krause, V. M. Mostepanenko, *Ann. Phys. (N.Y.)* **2005**, *318*,
37.

[9] D. Iannuzzi, M. Lisanti, F. Capasso, *Proc. Natl. Acad. Sci. USA* **2004**,
101, 4019.

[10] a) F. Chen, G. L. Klimchitskaya, V. M. Mostepanenko, U. Mohideen,
Opt. Express **2007**, *15*, 4823; b) F. Chen, G. L. Klimchitskaya,
V. M. Mostepanenko, U. Mohideen, *Phys. Rev. B* **2007**, *76*, 035338;
c) R. Castillo-Garza, C.-C. Chang, D. Jimenez, G. L. Klimchitskaya,
V. M. Mostepanenko, U. Mohideen, *Phys. Rev. A* **2007**, *75*, 062114.

[11] a) S. de Man, K. Heeck, R. J. Wijngaarden, D. Iannuzzi, *Phys. Rev.
Lett.* **2009**, *103*, 040402; b) G. Torricelli, I. Pirozhenko, S. Thornton,
A. Lambrecht, C. Binns, *Europhys. Lett.* **2011**, *93*, 51001.

[12] G. Torricelli, P. J. van Zwol, O. Shpak, C. Binns, G. Palasantzas,
B. J. Kooi, V. B. Svetovoy, M. Wuttig, *Phys. Rev. A* **2010**, *82*,
010101(R).

[13] a) F. Chen, U. Mohideen, G. L. Klimchitskaya, V. M. Mostepanenko,
Phys. Rev. A **2005**, *72*, 020101(R); b) F. Chen, G. L. Klimchitskaya,
V. M. Mostepanenko, U. Mohideen, *Phys. Rev. Lett.* **2006**, *97*,
170402.

[14] C.-C. Chang, A. A. Banishev, G. L. Klimchitskaya, V. M. Mostepanenko,
U. Mohideen, *Phys. Rev. Lett.* **2011**, *107*, 090403.

[15] D. Lencer, M. Salinga, B. Grabowski, T. Hickel, J. Neugebauer,
M. Wuttig, *Nat. Mater.* **2008**, *7*, 972.

[16] W. Wełnic, S. Botti, L. Reining, M. Wuttig, *Phys. Rev. Lett.* **2007**, *98*,
236403.

[17] S. R. Ovshinsky, *Phys. Rev. Lett.* **1968**, *21*, 1450.

[18] N. Yamada, E. Ohno, N. Akahira, K. Nishiuchi, K. Nagata, M. Takao,
Jpn. J. Appl. Phys. Part 1 **1987**, *26*, 61.

[19] H. IIwasaki, Y. Ide, M. Harigaya, Y. Kageyama, I. Fujimura, *Jpn. J.
Appl. Phys. Part 1* **1992**, *31*, 461.

[20] I. Satoh, N. Yamada, *Proc. SPIE* **2001**, *4085*, 283.

[21] E. R. Meinders, A. V. Mijritskii, L. van Pieterson, M. Wuttig, *Optical
Data Storage: Phase Change Media and Recording*, Springer, Berlin
2006.

[22] W. Y. Cho, S.-W. Jeong, F. Somenzi *IEEE J. Solid-State Circuits* **2005**,
40, 293.

[23] M. H. R. Lankhorst, B. W. S. M. M. Ketelaars, R. A. M. Wolters, *Nat.
Mater.* **2005**, *4*, 347.

[24] M. Wuttig, N. Yamada, *Nat. Mater.* **2007**, *6*, 824.

[25] B. Huang, J. Robertson, *Phys. Rev. B* **2010**, *81*, 1.

[26] a) T. Siegrist, P. Jost, H. Volker, M. Woda, C. Schlockermann,
P. Merkelbach, M. Wuttig, *Nat. Mater.* **2011**, *10*, 202; b) For charge
densities see also M. Woda, Ph.D Thesis, RWTH Aachen **2010**.

[27] K. Shportko, S. Kremers, M. Woda, D. Lencer, J. Robertson,
M. Wuttig, *Nat. Mater.* **2008**, *7*, 653.

[28] D. Lencer, M. Salinga, M. Wuttig *Adv. Mater.* **2011**, *23*, 2030.

[29] G. Bruns, P. Merkelbach, C. Schlockermann, M. Salinga, M. Wuttig,
T. D. Happ, J. B. Philipp, M. Kund, *Appl. Phys. Lett.* **2009**, *95*,
043108.

[30] J. Siegel, A. Schropp, J. Solis, C. N. Afonso, M. Wuttig, *Appl. Phy.
Lett.* **2004**, *84*, 2250.

[31] W. K. Njoroge, H. W. Woltgens, M. Wuttig, *J. Vac. Sci. Technol. A*
2002, *20*, 230.

[32] a) J. Z. Liu, P. C. Taylor, *Solid State Commun.* **1989**, *70*, 81; b) J. Z. Liu,
P. C. Taylor, *J. Non-Cryst. Solids* **1989**, *114*, 25.

[33] A. H. Edwards, A C. Pineda, *Phys. Rev. B* **2006**, *73*, 045210.

[34] V. B. Svetovoy, P. J. van Zwol, G. Palasantzas, J. Th. M. DeHosson,
Phys. Rev. B. **2008**, *77*, 035439.

[35] P. J. van Zwol, G. Palasantzas, J. Th. M. De Hosson *Phys. Rev. B*
2008, *77*, 075412.

[36] G. Torricelli, S. Thornton, C. Binns, I. Pirozhenko, A. Lambrecht,
J. Vac. Sci. Technol. B **2010**, *28*, C4A30.

[37] a) G. Palasantzas, P. J. van Zwol, J. Th. M. DeHosson, *Appl.
Phys. Lett.* **2008**, *93*, 121912; b) P. J. van Zwol, V. B. Svetovoy,
G. Palasantzas, *Phys. Rev. B* **2009**, *80*, 235401.

[38] P. J. van Zwol, G. Palasantzas, J. Th. M. DeHosson, V. Graig, *Lang-
muir* **2008**, *24*, 7528.

[39] G. Jourdan, A. Lambrecht, F. Comin, J. Chevrier, *Eur. Phys. Lett.*
2009, *85*, 31001.

[40] W. J. Kim, A. O. Sushkov, D. A. R. Dalvit, S. Lamoreaux, *Phys. Rev.
Lett.* **2009**, *103*, 060401.

[41] a) P. J. van Zwol, G. Palasantzas, *Phys. Rev. B* **2009**, *79*,
195428; b) P. J. van Zwol, G. Palasantzas, *Phys. Rev. E* **2009**, *79*,
041605; c) P. J. van Zwol, G. Palasantzas, *Phys. Rev. A* **2010**, *81*,
062502.

[42] A. Benassi, C. Calandra, *Eur. Phys. Lett.* **2008**, *84*, 11002.